

# 1 Arable soil nitrogen dynamics reflect organic 2 inputs via the extended composite phenotype, 3 not the metagenome associated with nitrogen 4 transformations.

5 **Andrew L. Neal<sup>1†</sup>, Harry A. Barrat<sup>1</sup>, Aurélie Bacq-Lebreuil<sup>2‡</sup>, Yuwei Qin<sup>3</sup>, Xiaoxian Zhang<sup>4</sup>,  
6 Taro Takahashi<sup>1,5</sup>, Valentina Rubio<sup>6,7</sup>, David Hughes<sup>8</sup>, Ian M. Clark<sup>4</sup>, Laura M. Cárdenas<sup>1</sup>,  
7 Laura-Jayne Gardiner<sup>9</sup>, Ritesh Krishna<sup>9</sup>, Margaret L. Glendining<sup>8</sup>, Karl Ritz<sup>2</sup>, Sacha J.  
8 Mooney<sup>2</sup>, John W. Crawford<sup>10</sup>.**

9 <sup>1</sup>Net Zero and Resilient Farming, Rothamsted Research, North Wyke, EX20 2SB, UK;

10 <sup>2</sup>School of Biosciences, The University of Nottingham, Sutton Bonington, LE12 5RD, UK;

11 <sup>3</sup>Department of Environmental Sciences, Wageningen University, 6700 HB Wageningen, The Netherlands;

12 <sup>4</sup>Sustainable Soils and Crops, Rothamsted Research, Harpenden, AL5 2JQ, UK;

13 <sup>5</sup>Bristol Veterinary School, University of Bristol, Langford, BS40 5DU, UK;

14 <sup>6</sup>Programa de Producción y Sustentabilidad Ambiental, Instituto Nacional de Investigación Agropecuaria  
15 (INIA), Estación Experimental INIA La Estanzuela, Colonia, Uruguay;

16 <sup>7</sup>School of Integrative Plant Science, Cornell University, Ithaca, NY 14853, USA;

17 <sup>8</sup>Intelligent Data Ecosystems, Rothamsted Research, Harpenden, AL5 2JQ, UK;

18 <sup>9</sup>IBM Research Europe - Daresbury, The Hartree Centre, Warrington, WA4 4AD, UK;

19 <sup>10</sup>Adam Smith Business School, University of Glasgow, Glasgow, G12 8QQ, UK.

20 <sup>†</sup>andy.neal@rothamsted.ac.uk; <sup>‡</sup>present address: Genesis, 4 rue de l'église, 27440, Lisors, France.

## 21 **Abstract**

22 Achieving food security whilst minimising agriculture's influence on climate and biodiversity  
23 requires resilient systems, predicated on improved nutrient-use efficiency, water and nutrient storage  
24 in soils and reducing gaseous emissions. Success requires sufficient understanding of coupled  
25 nitrogen and carbon metabolism in soils, associated influences on soil structure, and of processes  
26 controlling nitrogen-transformations at scales relevant to microbial activity. We show the influence  
27 of organic matter on arable soil nitrogen transformations and balances can be understood by  
28 integrating metagenomic data with soil structural parameters. System function can be predicted from  
29 theory of soil as an extended composite phenotype, where physical and biotic interactions result in

30 emergent organisation and function. The approach provides mechanistic explanation of why organic  
31 matter is effective in reducing nitrous oxide losses while supporting system resilience. The  
32 relationship between organic carbon, soil connected porosity and flow rates at scales relevant to  
33 microbes suggests significant increases in efficiency and resilience could be achieved at lower organic  
34 carbon stocks than currently envisaged.

## 35 **Main**

36 Agricultural production must balance ostensibly incompatible demands. Ideally, it must provide  
37 sufficient, nutritious food to increasing human populations, reduce its environmental footprint, restore  
38 biodiversity, and attenuate greenhouse gas (GHG) emissions and associated climate change. Soil is  
39 simultaneously the most important terrestrial sink and source of GHG, particularly the long-lived  
40 gases carbon dioxide and nitrous oxide (N<sub>2</sub>O), and shorter-lived methane<sup>1</sup>. As N<sub>2</sub>O constitutes a loss  
41 of an important plant nutrient from the system, nitrogen dynamics in soil are particularly important in  
42 linking climate regulation and food security<sup>2</sup>. Improving nutrient use efficiency (NUE) such that GHG  
43 emissions resulting from fertiliser production and use falls by 40% *per* unit of food produced is  
44 predicted to be more effective at reducing emissions from the food system than higher-yielding crops  
45 or a 50% reduction in food waste<sup>3</sup>. NUE and carbon sequestration, are closely coupled in soils<sup>4</sup>, co-  
46 regulated by microbial metabolism which, in turn, is governed by oxygen availability and co-location  
47 of nitrogen in, and together with, organic matter. The distribution of oxygen, in turn, is determined by  
48 the physical soil pore structure, its moisture content, and the distribution of potential microbial  
49 respiration<sup>5</sup>. Therefore, an understanding of how management impacts on the partitioning of carbon  
50 and nitrogen between storage in soil and emissions requires an understanding of the dynamics of  
51 both the physical and biotic state. The ‘*extended composite phenotype*’ theory of soil provides the  
52 required framework.

53 Important soil functions, particularly transport capacity, metabolic efficiency, and resource supply  
54 resilience to plants, acting across a broad range of scales, are dependent upon the connectivity and  
55 heterogeneity of pore space, emphasizing the importance of a pore-centric view of soil architecture<sup>6</sup>.

56 The theory of soil as an extended composite phenotype is based on detailed observations and  
57 modelling of the interactions between structural genesis and microbial community structure and  
58 function<sup>7</sup>. Soils exhibit spontaneous emergence of multi-scale self-organisation driven by endogenous  
59 feedback between pore space architecture and microbial metagenetic—rather than taxonomic—  
60 states<sup>7</sup>. Microbiological activity influences soil pore architecture at scales below approximately 80  
61  $\mu\text{m}$ . Since these are the scales that affect the relative balance and distribution of air and water in soil,  
62 these changes also influence the nature of microbial activity, especially the relative activity of aerobic  
63 and anaerobic metabolism. The resulting process-form state is a consequence of the self-organisation  
64 of the integrated biophysical system of soil<sup>7,8</sup>. The emergent state is affected by incorporation of OM  
65 into soil because this drives a tightly coupled feedback involving changes to the process-form state  
66 associated with altered gene assemblages and soil texture – hence the extended phenotype<sup>7-10</sup> of the  
67 soil system is an irreducible composite reflecting physical and biotic feedbacks.

68 Based upon our previous observations, the soil extended composite phenotype incorporates microbial  
69 gene assemblages, soil structural parameters, hierarchical flux processes of gases and water, and  
70 overall system function including the likelihood of anoxia. In soil with a high throughput of OM,  
71 process-form states are characterised as having a high porosity and a high degree of pore  
72 connectivity<sup>11,12</sup>. Reduced levels of OM are associated with less extensively developed soil pore  
73 networks. The resultant altered state modifies diffusivity and  $\text{O}_2$  permeability<sup>7,13-16</sup>. This pore-centric  
74 perspective is essential when considering the consequences of incorporating OM into arable soils for  
75 NUE and GHG emissions. The extended composite phenotype of soils containing low stocks of  
76 organic carbon is characterised by greater proportions of anoxic pore space—the principal control of  
77 biological denitrification activity<sup>17</sup>—and increased abundance of genes in the metagenome associated  
78 with dissimilatory respiration of nitrate and nitrite<sup>7</sup>. These factors effectively link the fates of nitrogen  
79 and carbon in soil.

80 Here, we provide a further test of the theory of soil as an extended composite phenotype, to provide a  
81 mechanistic explanation of the links between carbon and nitrogen metabolism and show how both  
82 physical and genetic factors must be accounted for. According to this theory, we hypothesise that  
83 arable soils receiving high organic inputs would have a highly connected process-form state resulting

84 in reduced losses of stored nitrogen as N<sub>2</sub>O through anaerobic metabolism. Conversely, soils  
85 receiving low organic inputs would result in a poorly connected state, reduced oxygen flux and higher  
86 gaseous losses of nitrogen. Furthermore, using this framework, we seek to explain the link between  
87 carbon dynamics and non-equilibrium NUE, calculated as the balance of nitrogen inputs, off-takes  
88 and accumulation in soil. We hypothesise that offsetting losses of N<sub>2</sub>O from soil would be associated  
89 with higher stocks of soil nitrogen, along with carbon and water storage—key factors in conveying  
90 resilience in rainfall-limited production systems. To test our hypotheses, we studied arable soils  
91 subjected to consistent management for over 160 years, comparing soils which had received a range  
92 of continuous organic or inorganic fertilisation over this period.

## 93 **Results and discussion**

### 94 **Emergent soil process-form states**

95 **Co-metabolism of carbon and nitrogen** – Since experiment establishment (1843), soils subject to  
96 different management or fertilisation (Table I) have developed distinct soil organic carbon (SOC) and  
97 total nitrogen (N<sub>tot</sub>) stocks (Supplementary Fig. 1). Woodland and proximal grassland soils, together  
98 with arable soil receiving composted farmyard manure (FYM) were the only soils to display net SOC  
99 and N<sub>tot</sub> accumulation (Fig. 1). Grassland and FYM-amended arable soils both contained over 70 Mg  
100 ha<sup>-1</sup> SOC and over 6 Mg ha<sup>-1</sup> N<sub>tot</sub>, significantly more than other treatments. There was a positive  
101 geometric mean functional relationship between SOC and N<sub>tot</sub> (Fig. 2), corresponding to a C:N ratio of  
102 11.4. Despite widely varying quantities and qualities of carbon and nitrogen inputs, this indicates  
103 coupling via the same metabolic pathways and mechanisms of storage in soil. Metabolic and storage  
104 constraints in soil are both linked to microenvironmental conditions, *via* a strong association between  
105 SOC inputs and soil process-form relationships<sup>7</sup>. Therefore, we quantified micrometre-scale structure  
106 of a subset of soils to understand the biophysical feedbacks in the co-metabolism of carbon and  
107 nitrogen.

108 **Links between nitrogen storage and physical processes** – Parameters relating to soil  
109 architecture were determined in grassland, woodland, FYM, and inorganically fertilised arable soils



110 receiving 144 kg-N ha<sup>-1</sup> yr<sup>-1</sup> as ammonium nitrate, phosphorus and potassium (<sup>144</sup>NPK), 192 kg-N ha<sup>-1</sup>  
111 yr<sup>-1</sup> and potassium but no phosphorus (<sup>192</sup>NK), and soil receiving no nitrogen fertilisation but  
112 phosphorus and potassium (PK). Significant treatment-dependant differences were observed for  
113 parameters generated directly from X-ray computed tomography of pore networks in each soil (total  
114 [P<sub>t</sub>] and connected [P<sub>c</sub>] porosity) and those derived from simulation of the permeability (*k*),  
115 normalized effective oxygen diffusion coefficient (*D<sub>e</sub>'*), and hydraulic conductivity (*K*) within the  
116 pore networks (Table II). Collectively, these measures describe the dynamical state of soil pore space  
117 and the maximum potential rate at which resources can move through the networks, *i.e.*, the capacity  
118 for flux. Grassland, woodland and FYM-amended arable soils were typified as having more extensive  
119 and more connected pore networks than inorganically fertilised arable soils. We observed a power-  
120 law relationship between P<sub>c</sub> and *K*: increased SOC was associated with increases in both parameters  
121 (Fig. 2B). Regions of this relationship correspond to the process-form states of the various soils. This  
122 infers that—in the case of the soils studied here—for P<sub>c</sub> between 0.05 and 0.4, relatively small  
123 changes in geometry, characterised by P<sub>c</sub>, result in substantial increases in *K*, characterising flow rate.  
124 This power law therefore has profound implications for soil management strategies.

125         The effect of soil management was most evident on permeability (*k*) based upon treatment  
126 effect size ( $\omega^2$ , Table II). We simulated the anoxic proportion of each soil across a range of matric  
127 potentials ( $\psi_m$ ). Addition of FYM to arable soils resulted in a matric potential–anoxic space profile  
128 distinct from inorganically fertilised arable soils (Fig. 2C). Inorganically fertilised <sup>192</sup>NK and <sup>144</sup>NPK  
129 soils, as well as soil that had received no fertilisation (referred to as *nil*, Table I) all presented large  
130 proportions of anoxic space under relatively dry conditions ( $\psi_m$  50–65 kPa) and were predicted to be  
131 completely anoxic at  $\psi_m$  between 38.4–32.0 kPa. In contrast, the process-form state of FYM-amended  
132 soil exhibited aspects of woodland and grassland soils. Under relatively dry conditions FYM soil had  
133 low proportions of anoxic space more typical of grassland soil. At increased moisture content, both  
134 soils were completely anoxic at 22.6 kPa; woodland soil being so at 20.2 kPa.

135         As with an affiliated ley-arable experiment<sup>7</sup>, organic-carbon rich soil developed a distinct  
136 process-form state, typified by a greater proportion of connected pores, and increased hydraulic  
137 conductivity (Fig. 2B). Modelling predicts this to be a more oxygenated pore network (Fig. 2C) by

138 virtue of its greater capacity to transport O<sub>2</sub>. Annual addition of FYM (35 Mg ha<sup>-1</sup>) to the soil has  
139 resulted in SOC and N<sub>tot</sub> contents, and process-form states resembling unmanaged woodland and  
140 grassland, despite regular physical disturbance by inversion tillage. This combined evidence is  
141 consistent with our hypothesis regarding the influence of organic carbon in soils in creating a more  
142 highly connected and oxygenated structure.

143 **Consequences of soil processes-form state for potential biological function** – Nitrogen  
144 transformation-associated metagenomes were determined in grassland, woodland, FYM, <sup>144</sup>NPK,  
145 <sup>192</sup>NK and PK soils from shotgun metagenomic approaches. There was a significant treatment effect  
146 upon gene assemblages (PERMANOVA, 99,999 permutations: *pseudo-F*<sub>5,12</sub>=22.5, *p*<sub>perm</sub>=1x10<sup>-5</sup>).  
147 *Post hoc* pairwise comparisons indicated no significant difference in gene assemblages between <sup>192</sup>NK  
148 and PK soils. All other comparisons were significantly different.

149 Hierarchical clustering of soils based upon centred log-ratio transformed counts of read  
150 numbers matching each identified gene (*i.e.*, relative abundance) demonstrated gene assemblages of  
151 unmanaged woodland and grassland soils were distinct from arable soils (Fig. 3). Genes separated  
152 into two broad clusters based upon their distribution between unmanaged and arable soils. The first  
153 included genes associated with amino-acid metabolism and other nitrogen-assimilation pathways,  
154 including nitrate assimilation (KEGG module M00615) and assimilatory nitrate reduction (M00531).  
155 Several genes associated with dissimilatory nitrate reduction (M00530) and denitrification (M00529)  
156 were also associated with this cluster. Relative abundance of these genes was greater in woodland  
157 and grassland soils—which were most alike—than arable soils (Fig. 3). More subtly, genes  
158 associated with nitrate assimilation were relatively more abundant in FYM-amended than  
159 inorganically fertilised arable soils.

160 The second gene cluster was generally more abundant in arable soils. This comprised genes  
161 associated with several modules, including nitrification (M00528), denitrification (M00529),  
162 dissimilatory nitrate reduction (M00530) and complete nitrification (M00804), (*c.f.* Supplementary  
163 Information). This pattern of limited genotypic differences between arable soils is broadly consistent  
164 with known responses of microbial communities to nitrogen fertilisation<sup>18-21</sup>. This is evidence for

165 direct influence of process-form states upon nitrogen-associated gene assemblages in soil, particularly  
166 the association of nitrogen assimilatory pathways with soils having the greatest SOC and  $N_{tot}$ ,  
167 connected porosity, and hydrodynamic conductivity. The greater relative abundance of genes  
168 associated with nitrogen assimilation in FYM-amended soil is consistent with this soil having a  
169 similar process-form state (Fig. 2B) and oxygen status (Fig. 2C) to woodland and grassland soils.  
170 Soils having low SOC (and  $N_{tot}$ ) and thus low connected porosity and hydrodynamic conductivity  
171 were associated more with dissimilatory pathways, utilizing oxidised forms of nitrogen as alternative  
172 electron acceptors for respiration. Within arable plots particularly, there was a subtle shift in genes  
173 associated with denitrification and dissimilatory nitrate reduction: NO-forming and cytochrome *c*-type  
174 nitrate reductases (*nirK* and *napAB* respectively) were relatively more abundant in FYM-amended  
175 than inorganically fertilised soils. These genes are typically associated with more oxygenated  
176 environments than the functionally equivalent but structurally dissimilar genes *nirS* (*c*-type  
177 cytochrome) and the nitrite oxidoreductase *nxrAB*<sup>22-25</sup> and were most abundant in grassland and  
178 woodland soils respectively. In addition, FYM had the highest relative abundance of genes of the  
179 high-affinity nitrate-binding transporter (*nrtABC*) of all arable soils. These genes were otherwise  
180 most abundant in grassland soils. Nitrite reductases typical of more reducing environments (*nirS*,  
181 *nxrAB*) were indicative of arable soils in general, particularly <sup>144</sup>NPK, <sup>192</sup>NK treatments. In FYM-  
182 amended soil, the more oxygen-rich process-form state (Fig. 2C) influences the gene assemblage such  
183 that it shares similarities to those of grassland and woodland soils.

184 Assessment of gene abundance associated with nitrogen transformations by quantitative PCR provides  
185 evidence of the pattern and rate of nitrogen cycling processes in soil<sup>26</sup>. However, the relative  
186 abundance of different genes discussed above (and Supplementary Information) generated from  
187 metagenomics cannot in themselves be used as the basis for estimates of process rates<sup>27</sup>. We assumed  
188 relative gene abundance reflects the *likelihood of a process* with which they are associated when  
189 environmental conditions allow. To test this assumption, we measured N<sub>2</sub>O emissions in the field,  
190 relating them to relative gene abundance and predictions of anoxic pore space (Fig. 2c).

191 **Nitrous oxide emissions from soil** – Since lower levels of organic carbon are associated with less  
192 extensively-developed soil pore networks<sup>11,12</sup> (Table II) and the resultant low diffusivity restricts  
193 oxygen permeability<sup>7,13-16</sup> (Fig. 2C), elevated N<sub>2</sub>O emissions are often associated with poor soil  
194 architecture. We placed static chambers<sup>28</sup> in the field on FYM, <sup>240</sup>NPK, <sup>192</sup>NK, <sup>144</sup>NPK and PK soils  
195 between April and November 2019 to compare soil N<sub>2</sub>O emissions. For each measurement date,  
196 greatest emissions were typically measured from <sup>240</sup>NPK soils and least from PK soils  
197 (Supplementary Fig. 2). We detected no significant influence of soil temperature (ANCOVA;  
198  $F_{1,134}=0.901$ ,  $p=0.344$ ) or potential soil moisture deficit (ANCOVA;  $F_{1,134}=0.272$ ,  $p=0.603$ ) upon N<sub>2</sub>O  
199 emissions. Comparing soils directly, there was a significant influence of arable soil management  
200 (ANOVA;  $F_{4,116}=8.7$ ,  $p=3\times 10^{-6}$ ) upon soil mean daily N<sub>2</sub>O emission (Fig. 4). FYM-amended soil  
201 emitted significantly less N<sub>2</sub>O than <sup>240</sup>NPK soil ( $t=3.1$ ;  $p=0.005$ ), despite receiving similar annual  
202 nitrogen inputs and having more than double the nitrogen stocks of inorganically fertilised soils  
203 (Supplementary Fig. 1).

204 **Non-equilibrium nitrogen use efficiency of the soil-plant system** – We hypothesised that  
205 differences in extended composite phenotype of FYM-amended and inorganically fertilised arable soils  
206 would be reflected in historical nitrogen fluxes and stocks through the soil-plant systems. Traditionally,  
207 NUE is expressed as a ratio between the amount of nitrogen introduced to and harvested from a system  
208 within a single season<sup>29-31</sup>. This implicitly assumes a system is operating under a long-term equilibrium,  
209 where soil nitrogen stocks remain temporally constant. For the inorganically fertilised plots this  
210 condition is largely satisfied, due to the long trial history meaning annual production of soil organic  
211 nitrogen virtually equals annual nitrogen mineralisation<sup>32,33</sup>. However, when this condition is not  
212 satisfied—FYM-amended soils continue to accumulate nitrogen (Fig. 1B)—applied nitrogen stored in  
213 soil beyond a single cropping cycle is incorrectly considered ‘wasted’. Although nitrogen which  
214 accumulates in soil is not recovered by the immediate crop, it may contribute to system resilience by  
215 supporting production of subsequent crops. To account for this, we calculated non-equilibrium NUE  
216 for treatments, apportioning nitrogen introduced to each system between that taken up by the crop,  
217 stored in soil and ‘lost’ from the soil-plant system. For lost nitrogen, gaseous losses resulting from

218 denitrification may be up to double those via leaching<sup>34</sup>. Since <sup>240</sup>NPK and FYM receive similar levels  
219 of nitrogen inputs (but differ in levels of readily available nitrogen), the effect of organic carbon input  
220 can be evaluated. Mean annual nitrogen fluxes through the three pools following addition to the  
221 different winter wheat crop systems (2000-2015) demonstrate progressively greater losses of nitrogen  
222 inputs with increasing fertilisation (Fig. 5A). Whilst total nitrogen associated with wheat grain and  
223 straw increases as nitrogen inputs increase, the proportion of total assimilated nitrogen reduces  
224 (Supplementary Fig. 3), indicating progressively reduced long-term NUE. Nitrogen inputs required to  
225 generate a 1 Mg grain harvest show similar trends (Fig. 5B). Set alongside inorganically fertilised  
226 systems, and particularly <sup>240</sup>NPK, the FYM system shows altered allocation of added nitrogen to each  
227 pool. Reduced total (Fig. 5A) and proportional (Supplementary Fig. 3) allocation of nitrogen to lost  
228 pools and increased in nitrogen stocks (*cf.* Figs. 1 and 5A), suggest greater NUE. This increased  
229 efficiency is tempered by reduced nitrogen allocation to crops and grain yields (Fig. 5). The 2000-2015  
230 average grain yield from FYM-amended soil was 1.1 Mg ha<sup>-1</sup> less than from <sup>240</sup>NPK fertilised soil  
231 ( $Q=4.2$ ;  $p=0.035$ ). This is consistent with lower area-scaled (but greater yield-scaled) N<sub>2</sub>O emissions  
232 from soils receiving organic amendments rather than inorganic fertiliser<sup>35</sup>. Measured and simulated  
233 micropore-scale behaviour of soil extended composite phenotypes reflect our field-scale description of  
234 nonequilibrium NUE, particularly reductions in the absolute and proportional size of the lost nitrogen  
235 pool. Our data suggest that the application of FYM to soil is directly related to the reduction of nitrogen  
236 losses since we observe a 1.5-fold increase in soil P<sub>t</sub> and a four-fold increase in  $k$  in FYM-amended  
237 over inorganically fertilised soils.

238 **The extended composite phenotype and system resilience** - Consistent with our hypothesis that  
239 nitrogen balance in soils would be altered under different emergent process-form states, we observe that  
240 the reduced area-scaled N<sub>2</sub>O emissions in FYM amended soils associated with high connected porosity  
241 and predicted greater oxygen availability are associated with greater N<sub>tot</sub> stocks over the long term. By  
242 combining physical structure with metagenetic and phenotypic description, we invoke a more  
243 fundamental and mechanistic conceptualisation of the role of organic matter in soil function. We  
244 demonstrate that the nitrogen-associated metagenome responds to nitrogen fertilization markedly, but

245 that form of nitrogen input exerts relatively little influence upon redox sensitive *nirK-napAB* and *nirS-*  
246 *nxrAB* gene abundances. Given the magnitude of the changes we observe in process-form state, it is  
247 likely that OM controls N<sub>2</sub>O emissions by influencing gene expression (phenotype) rather than altering  
248 gene abundance (genotype). In effect, reduced nitrous oxide losses are a co-benefit of increased organic  
249 inputs. This regulation results in nitrogen accumulation in soil conferring a degree of resilience,  
250 consistent with previously observed reductions in the need for inorganic nitrogen application to achieve  
251 a target yield in organic carbon-rich soils<sup>36</sup>. Evidence for higher SOC stocks being associated with  
252 higher crop yields is equivocal<sup>37-38</sup>. However, resilience of rainfed crop yields to drought does appear  
253 to be related to higher SOC stocks<sup>39,40</sup>, although in the soils studied here such effects are only observed  
254 where nitrogen availability limits crop yield<sup>41</sup>.

255 **Conclusions** -- Soil presents a multivariate conundrum in which simple, linear cause-effect  
256 processes—however conceptually appealing—are difficult to reconcile with field data. Our adoption  
257 of a novel non-linear and systems-level approach, founded on quantification of the process-form state  
258 and interactions with the metagenome, shows that the behaviour of the soil system cannot be understood  
259 by studying the behaviour of the physical and biotic components in isolation. Our emphasis is on a  
260 parsimonious explanation for our observations. It shows that the form of nitrogen fertilisation in arable  
261 systems does little to influence nitrogen-metabolism-associated gene assemblages, but control over  
262 expression is exerted by the emergent process-form state which is dependent upon organic matter  
263 inputs. Combined evidence suggests a mechanistic basis for why regular addition of organic matter to  
264 arable soils is effective in reducing losses of nitrogen as N<sub>2</sub>O to the atmosphere. Whilst the applications  
265 of FYM used in our experimental system are impractical<sup>42</sup>, the power-law relationship observed in Fig.  
266 2 implies that similar levels of efficiency and resilience could be achieved at lower SOC input and  
267 stocks than used here. One consequence of close coupling of carbon and nitrogen metabolism is that  
268 increased N<sub>2</sub>O emissions may offset any benefits for limiting global warming accruing from actively  
269 increasing SOC stocks<sup>43,44</sup>. Our data suggest that optimally efficient systems can achieve both increased  
270 SOC stocks and reduced N<sub>2</sub>O emissions. The extended composite phenotype concept provides an

271 integrative explanation why this might be so, based upon a biological and pore-centric understanding  
272 of soil processes.

## 273 **Methods**

274 **Field experiment and soil sampling** – Soil used to generate physical data relating to soil  
275 structure and biological data derived from metagenomics was sampled from arable soils which had  
276 received inorganic fertiliser inputs ranging from no inputs to different combinations of inorganic  
277 nitrogen (ammonium nitrate), phosphorus and potassium, comparing rates of nitrogen inputs from 0 to  
278 240 kg ha<sup>-1</sup> yr<sup>-1</sup> from contrasting treatments of the Broadbalk Long-Term field experiment established  
279 in 1843 (51°48'35" N, 00°22'30" W). The experiment tests the long-term consequences of different  
280 fertiliser and manure applications on the yield of winter wheat, as well as the effect of cessation of all  
281 cultivation from a part of the site in 1882. Detailed description of the treatments compared in this  
282 study are provided in the Supplementary Information: comprehensive details regarding the experiment  
283 history are provided by Macdonald *et al.*<sup>45</sup>. We also studied two soils which had not been subject to  
284 management for over a century: part of the original Broadbalk experiment which since 1882 has been  
285 allowed to revert naturally to a woodland (referred to as the woodland treatment), and plots of the  
286 Highfield Ley-Arable experiment managed as a mown sward<sup>45</sup> (referred to as the grassland  
287 treatment). Details of the management associated with the different soils compared in his work are  
288 provided in Table I. Treatments are not replicated across the Broadbalk experiment. Therefore,  
289 samples associated with metagenomics and X-ray computed tomography (both described below) are  
290 by necessity *pseudo*-replicates. Assessment of differences between treatments as a consequence are  
291 relative to the pooled within-plot variability in both ANOVA and PERMANOVA tests, rather than  
292 some form of between-plot variability, and we cannot statistically separate spatial from “treatment”  
293 effects. Our approach therefore tests the hypothesis that there are differences in measured and  
294 simulated soil parameters, and assemblages and relative abundance of nitrogen cycle-associated genes  
295 in the different plots at the Broadbalk site. We cannot conclude, based on statistical inference, that any  
296 differences observed result from different fertility management directly. However, it is reasonable to  
297 interpret our observations of between-plot differences in soil structure and relative gene abundance

298 within the context of the broader data relating to SOC and  $N_{\text{tot}}$  stocks, held by the *e*-RA electronic  
299 database, and  $N_2O$  emissions—all of which are temporally replicated—to suggest explanations for the  
300 patterns we observe.

### 301 **Soil structure and hydrodynamic behaviour**

302 **X-ray computed tomography and image analysis** – We generated X-ray CT images from grassland,  
303 woodland, FYM,  $^{144}\text{NPK}$ ,  $^{192}\text{NK}$  and nil treatments at 1.5  $\mu\text{m}$  resolution and scales relevant to  
304 microbes ( $10^0$ - $10^2$   $\mu\text{m}$ ), requiring imaging of 0.7 – 2.0 mm diameter soil aggregates. Aggregates ( $n$   
305 = 9) were selected at random from soil collected from each plot. Each was scanned using a Phoenix  
306 Nanotom system (GE Measurement and Control solution, Wunstorf, Germany) operated at 90 kV, a  
307 current of 65  $\mu\text{A}$  and at a voxel resolution of 1.5  $\mu\text{m}$ . Initial image analysis was performed using  
308 Image-J. Images were threshold-adjusted using a bi-level bin approach<sup>47</sup> using QuantIm version 4.01.  
309 Porosity was calculated directly from threshold-adjusted binary images, pore connectivity was  
310 determined according to Vogel *et al.*<sup>47</sup>.

311 **Pore network permeability, hydraulic conductivity and oxygen diffusion in soil** – The  
312 permeability ( $k$ ) and hydraulic conductivity ( $K$ ) of soil pore networks, and the effective diffusion  
313 coefficient ( $D_e$ ) for oxygen within the pores was calculated for each soil structure imaged by X-ray  
314 CT using lattice Boltzmann simulation<sup>47,48</sup>. Permeability and hydraulic conductivity were calculated  
315 as described by Zhang *et al.*<sup>15</sup>. For oxygen diffusion, hierarchical soil structures revealed by X-ray  
316 CT images indicate that gaseous oxygen in the atmosphere moves into soil primarily through its inter-  
317 aggregate pores and is then dissolved in water prior to moving into aggregates, largely by molecular  
318 diffusion. Since gaseous oxygen diffuses up to  $10^3$ -fold more quickly than oxygen dissolved in water,  
319 microbial community activity is constrained mainly by oxygen diffusion within aggregates. The  
320 ability of aggregates to conduct dissolved oxygen and other soluble substrates depends on the intra-  
321 aggregate pore geometry, and we quantified it with effective diffusion coefficients calculated directly  
322 by mimicking solute movement through the pore geometry using numerical simulations. The  
323 movement of solutes, including oxygen, within the pore geometry is assumed to be diffusion  
324 dominated. To account for the effect of temperature upon diffusion, we calculated a normalized



325 effective diffusion coefficient  $D_e'$  dividing the effective diffusion coefficient by the molecular  
326 diffusion coefficient of oxygen,  $D$ , in water at the same temperature, *i.e.*,  $D_e' = D_e/D$ <sup>15,16</sup>. Detailed  
327 description of pore-scale simulation is provided in the Supplementary Information.

328 **Modelling anoxia within soils** – Having established  $D_e'$  for oxygen in the soil pore networks of each  
329 soil, we simulated oxygen consumption by microbes under various levels of water saturation<sup>7</sup>. The  
330 first step of simulation was to determine water distributions in the pore networks under different  
331 matric potentials ( $\psi_m$ ). Once water distributions were determined for a given  $\psi_m$ , we simulated  
332 oxygen dissolution at air-water interfaces and then diffusion towards solid-water interfaces where it  
333 was reduced by microbial respiration. Microbial consumption was assumed to occur in water-filled  
334 voxels adjacent to the water-solid wall and described by a Monod kinetic equation. Oxygen diffusion  
335 and reduction was simulated to steady state. As the development of anaerobic volume is a balance  
336 between oxygen diffusion within the pore network and microbial consumption, we simulated two  
337 scenarios: fast ( $k' = 1 \times 10^{-2}$ ) and slow ( $k' = 1 \times 10^{-4}$ ) microbial consumption of oxygen to determine  
338 whether the relative anaerobicity of soils under the same  $\psi_m$  was a consequence of their structures and  
339 not microbial respiration rate. Once each system had reached a steady state, we considered sites where  
340 concentration of dimension-less dissolved oxygen was less than 20% to be anaerobic<sup>49</sup>. We repeated  
341 the procedure to achieve different water distributions calculated by varying  $\psi_m$  and then calculated the  
342 proportional change in the volumetric anaerobic sites with the  $\psi_m$  for both the fast and slow microbial  
343 reactions. Detailed description of these steps is provided in the Supplementary Information.

344 **DNA extraction, sequencing and quality control** – Three *pseudo*-replicate samples of soils  
345 from the grassland, woodland, FYM, <sup>144</sup>NPK, <sup>192</sup>NK and PK treatments were sampled in October  
346 2015. Soil community DNA was extracted from a minimum of 2 g of thawed soil the using MoBio  
347 PowerSoil DNA isolation kits (Mo Bio Laboratories, Inc. Carlsbad, CA). 10  $\mu$ g of high-quality DNA  
348 was provided for sequencing for each of the samples. Shotgun metagenomic sequencing of DNA was  
349 performed using 150-base paired-end chemistry on an Illumina HiSeq 2500 sequencing platform by  
350 Beijing Novogene Bioinformatics Technology Co. Ltd. (Beijing, China). The generated raw

351 sequences were limited to a minimum quality score of 25 and a minimum read length of 70 bases  
352 using Trimmomatic<sup>50</sup>.

353 **Bioinformatic analysis of metagenome sequences** - To assess general abundance of genes in  
354 metagenomes, we mapped individual metagenomic sequences to the RefSeq non-redundant (NR)  
355 protein database held at NCBI (downloaded August 22<sup>nd</sup>, 2018) using DIAMOND version 0.8.27<sup>53</sup> in  
356 BLASTX mode imposing a bitscore cut-off of 55. For each sequence, only the match with the highest  
357 bitscore was considered. Sequences not matching the NR database were considered currently  
358 unclassified. MEGAN Ultimate version 6.10.2<sup>52</sup> was used to associate metagenome sequences with  
359 Kyoto Encyclopaedia of Genes and Genomes<sup>53</sup> (KEGG) functional orthologs (ko) and modules (M).  
360 From all the reads binned to at least one KEGG orthologous group, we selected those associated with  
361 nitrogen metabolism (ko00910), amino acid metabolism (ko09105) and metabolism of other amino  
362 acids (ko09106) for detailed study of distribution differences between soils. Nitrous oxide is a  
363 product of autotrophic and heterotrophic nitrification pathways as well as denitrification. Emission  
364 rates differ markedly, both between processes and at different soil saturations<sup>54</sup>. Emission rates of  
365 N<sub>2</sub>O due to denitrification are far greater than from either nitrification pathway<sup>54</sup>. Not only is  
366 nitrification a minor source of N<sub>2</sub>O, but arable systems also exhibit the lowest maximum potential  
367 nitrification-derived N<sub>2</sub>O emissions across a broad range of ecosystems, and this declines with  
368 increasing management intensity<sup>55</sup>. For these reasons, we assumed that N<sub>2</sub>O emissions were  
369 predominantly driven by the influence of oxygen upon anaerobic respiration *via* the denitrification  
370 pathway. For each module in the KEGG ontology, genes may be associated with several sub-modules.  
371 These are not formed of exclusive sets of genes and so are likely to reflect a range of function and  
372 ecophysiology. In addition, the ontology does not distinguish between *amoABC* associated with  
373 nitrification and *pmoABC* associated with methane oxidation. Details of individual genes included in  
374 the analysis is provided in the Supplementary Information and the distribution of genes across  
375 different modules are shown in Fig. 3.

376 **Emissions of nitrous oxide from soil** – All nitrogen fertilisers were applied on April 12<sup>th</sup>, 2019,  
377 FYM was applied 17<sup>th</sup> September 2018 and 23<sup>rd</sup> September 2019. Measurement of gaseous emissions

378 from <sup>240</sup>NPK, FYM and PK soils were taken on eleven dates between April 11<sup>th</sup> and October 7<sup>th</sup>, 2019.  
379 Measurements from <sup>144</sup>NPK and <sup>192</sup>NK soils were taken on eight dates between April 23<sup>rd</sup> and October  
380 7<sup>th</sup>, 2019. Gas sampling was performed using in-field static chambers<sup>28</sup>. Three chambers (dimensions  
381 40 cm x 40 cm x 25 cm height) were inserted to a depth of 5 cm in soil of each treatment. Details of  
382 sampling times and frequency are provided in the Supplementary Information. N<sub>2</sub>O concentrations in  
383 gas samples collected in the field were analysed on a PerkinElmer Clarus 500 Gas Chromatograph  
384 (GC) equipped with a TurboMatrix 110 automated headspace sampler, fitted with an electron capture  
385 detector set at 300 °C for N<sub>2</sub>O analysis. The static chamber approach used here is prone to errors  
386 derived from GC instrumental noise and temperature and pressure changes within the chamber  
387 leading to artefactual negative fluxes of N<sub>2</sub>O<sup>56</sup>. To avoid these artefacts, only non-zero flux estimates  
388 were used to analyse differences in N<sub>2</sub>O emissions between treatments: negative fluxes were removed  
389 from the analysis. We summed total N<sub>2</sub>O emissions and tested for differences in the mean N<sub>2</sub>O  
390 emissions between treatments for the sampling period assessed on an area basis per day.

391 **Non-equilibrium nitrogen use efficiency of the soil-plant system** – The balance of nitrogen  
392 inputs, off-takes in wheat grain and straw and accumulation in arable soils was estimated for FYM,  
393 <sup>240</sup>NPK, <sup>192</sup>NPK, <sup>144</sup>NPK and PK Broadbalk fertiliser treatments between 2000 and 2015. Historical  
394 data relating to nitrogen inputs (as ammonium nitrate fertiliser or FYM, within seed grain and  
395 atmospheric deposition), off-takes (as harvested grain and straw), and soil nitrogen stocks were  
396 acquired from the *e*-RA managed database of data from Rothamsted's long-term experiments (data  
397 available from <http://doi.org/10.23637/rbk1-yldS10115-01>). The end-of-season fate of annual  
398 nitrogen additions in the form of inorganic fertiliser or FYM introduced to the Broadbalk continuous  
399 wheat plots was separated into three pools: (1) that taken up for the current season's production (*i.e.*  
400 nitrogen content in straw and harvested grain); (2) the pool held within the system for potential use in  
401 the future (*i.e.* change in soil nitrogen stock); and (3) that lost from the system without being utilised  
402 (*e.g.* as N<sub>2</sub>O emitted to the atmosphere or nitrate leached to groundwater). The agronomic  
403 performance of each plot was then evaluated by nonequilibrium nitrogen use efficiency, here defined  
404 as the ratio between nitrogen input and (1)+(2) above.

## 405 **Availability of data**

406 Data relating to the Broadbalk and Highfield long-term experiments can be accessed *via* the electronic  
407 Rothamsted Archive (<http://www.era.rothamsted.ac.uk/experiment/rbk1> and  
408 <http://www.era.rothamsted.ac.uk/experiment/rrn1>, respectively). Historical data relating to nitrogen  
409 inputs (as ammonium nitrate fertiliser or FYM, within seed grain and atmospheric deposition), off-  
410 takes (as harvested grain and straw), and soil nitrogen stocks are available from  
411 <http://doi.org/10.23637/rbk1-yldS10115-01>. All soil images are available upon reasonable request  
412 from the corresponding author. Code relating to lattice Boltzmann simulation is available upon  
413 request from Xiaoxian Zhang, Rothamsted Research. Sequence data associated with this research  
414 have been deposited in the European Nucleotide Archive  
415 <https://www.ebi.ac.uk/ena/browser/view/PRJEB43407?show=reads>.

## 416 **Acknowledgements**

417 This research was supported by UK Research and Innovation's (UKRI) Biotechnology and Biological  
418 Science Research Council (BBSRC)-funded Soil to Nutrition strategic program (BBS/E/C/000I0310  
419 and BBS/E/C/000I0320). The Broadbalk Wheat Experiment is part of the Rothamsted Long-term  
420 Experiments National Capability supported by BBSRC (BBS/E/C/000J0300) and the Lawes  
421 Agricultural Trust. LJG and RK were supported by the Hartree National Centre for Digital Innovation,  
422 a collaboration between UKRI's Science and Technology Facilities Council and IBM Research Europe.  
423 The authors are grateful to four anonymous reviewers for their time taken to provide helpful and  
424 encouraging comments on the original version of the manuscript. Their inputs have resulted in a much-  
425 improved text.

## 426 **References**

- 427 1. Laborde, D., Mamun, A., Martin, W. *et al.* (2021). Agricultural subsidies and global greenhouse  
428 gas emissions. *Nat. Commun.* 12, 2601.
- 429 2. Bouwman A.F., Boumans L.J.M., Batjes N.H. (2002). Emissions of N<sub>2</sub>O and NO from fertilized  
430 fields: summary of available measurement data. *Global Biogeochem. Cycles* 16, 1058-1070.
- 431 3. Clark M.A., Domingo N.G.G., Colgan K., *et al.*, (2020). Global food system emissions could  
432 preclude achieving the 1.5° and 2 °C climate change targets. *Science* 370, 705-708.
- 433 4. Guenet, B, Gabrielle, B, Chenu, C, *et al.* (2020). Can N<sub>2</sub>O emissions offset the benefits from soil  
434 organic carbon storage? *Global Change Biol.* 27: 237– 256.
- 435 5. Rappoldt C., Crawford J.W. (1999). The distribution of anoxic volume in a fractal model of soil.  
436 *Geoderma* 88, 329-347.
- 437 6. Letey, J. (1991). The study of soil structure - science or art. *Austr. J. Soil Res.* 29, 699–707.
- 438 7. Neal, A.L., Bacq-Labreuil, A., Zhang, X. *et al.* (2020). Soil as an extended composite phenotype  
439 of the microbial metagenome. *Sci. Rep.* 10, 10649.
- 440 8. Phillips, J.D. (2009). Soils as extended composite phenotypes. *Geoderma* 149, 142–151.

- 441 9. Dawkins, R. *The Extended Phenotype. The Gene as the Unit of Selection* (Oxford University  
442 Press, Oxford, 1982).
- 443 10. Dawkins, R. (2004). Extended Phenotype—but not too extended. A reply to Laland, Turner and  
444 Jablonka. *Biol. Philos.* 19, 377–396.
- 445 11. Schjønning, P., Munkholm, L.J., Moldrup, P. *et al.*, (2002). Modelling soil pore characteristics  
446 from measurements of air exchange: the long-term effects of fertilization and crop rotation. *Euro.*  
447 *J. Soil Sci.* 53, 331–339.
- 448 12. Bacq-Labreuil, A., Crawford, J., Mooney, S.J., *et al.*, (2018). Effects of cropping systems upon  
449 the three-dimensional architecture of soil systems are highly contingent upon texture. *Geoderma*  
450 332, 73–83.
- 451 13. Arah, J.R.M., Ball, B.C. (1994). A functional model of soil porosity used to interpret  
452 measurements of gas diffusion. *Euro. J. Soil Sci.* 45, 135–144.
- 453 14. Ball, B.C. (2013). Soil structure and greenhouse gas emissions: a synthesis of 20 years of  
454 experimentation. *Euro. J. Soil Sci.* 64, 357–373.
- 455 15. Zhang, X., Gregory, A.S., Whalley, W.R., *et al.*, (2021). Relationship between soil carbon  
456 sequestration and the ability of soil aggregates to transport dissolved oxygen. *Geoderma*, 403,  
457 115370.
- 458 16. Zhang, X., Neal, A.L., Crawford, J.W., *et al.*, (2021). The effects of long-term fertilizations on  
459 soil hydraulic properties vary with scales. *J. Hydrol.* 593, 125890.
- 460 17. Tiedje, J.M. (1988). Ecology of denitrification and dissimilatory nitrate reduction to ammonium,  
461 in *Biology of Anaerobic Microorganisms*, edited by A. J. B. Zehnder, pp. 179–244, John Wiley,  
462 New York.
- 463 18. Ramirez K.S., Lauber C.L., Knight R., *et al.*, (2010). Consistent effects of nitrogen fertilization  
464 on soil bacterial communities in contrasting systems. *Ecology* 91, 3463–3470.
- 465 19. Fierer N, Lauber CL, Ramirez KS, *et al.*, (2012). Comparative metagenomic, phylogenetic and  
466 physiological analyses of soil microbial communities across nitrogen gradients. *ISME J.* 6, 1007–  
467 1017.
- 468 20. Geisseler D., Scow K.M. (2014). Long-term effects of mineral fertilizers on soil microorganisms:  
469 a review. *Soil Biol. Biochem.* 75, 54–63.
- 470 21. Ouyang Y., Evans S.E., Friesen M.L., *et al.*, (2018). Effect of nitrogen fertilization on the  
471 abundance of nitrogen cycling genes in agricultural soils: a meta-analysis of field studies. *Soil*  
472 *Biol. Biochem.* 127, 71–78.
- 473 22. Knapp, C., Dodds, W. K., Wilson, K. C., *et al.*, (2009). Spatial heterogeneity of denitrification  
474 genes in a highly homogeneous urban stream. *Environ. Sci. Technol.* 43, 4273–4279.
- 475 23. Graham, D. W., Trippett, C., Dodds, W. K., *et al.* (2010). Correlations between in situ  
476 denitrification activity and *nir*-gene abundances in pristine and impacted prairie streams.  
477 *Environ. Poll.* 158, 3225–3229.
- 478 24. Tatariw, C., Chapman, E. L., Sponseller, R. A., *et al.*, (2013). Denitrification in a large river:  
479 consideration of geomorphic controls on microbial activity and community structure. *Ecology* 94,  
480 2249–2262.
- 481 25. Marchant, H., Ahmerkamp, S., Lavik, G. *et al.* (2017). Denitrifying community in coastal  
482 sediments performs aerobic and anaerobic respiration simultaneously. *ISME J.* 11, 1799–1812.
- 483 26. Petersen, D.G., Blazewicz, S.J., Firestone, M., *et al.*, (2012), Abundance of microbial genes  
484 associated with nitrogen cycling as indices of biogeochemical process rates across a vegetation  
485 gradient in Alaska. *Environ. Microbiol.* 14, 993–1008.
- 486 27. Rocca, J., Hall, E., Lennon, J. *et al.* (2015). Relationships between protein-encoding gene  
487 abundance and corresponding process are commonly assumed yet rarely observed. *ISME J.* 9,  
488 1693–1699.
- 489 28. Chadwick D.R., Cárdenas L., Misselbrook T.H., *et al.*, (2014). Optimizing chamber methods for  
490 measuring nitrous oxide emissions from plot-based agricultural experiments. *Euro. J. Soil Sci.*  
491 65, 295–307.
- 492 29. Raun W.R., Johnson G.V. (1999). Improving nitrogen use efficiency for cereal production.  
493 *Agron. J.* 91, 357–363.
- 494 30. Erisman JW, Leach A, Bleeker A, *et al.*, (2018). An integrated approach to a nitrogen use  
495 efficiency (NUE) indicator for the food production–consumption chain. *Sustainability* 10, 925

- 496 31. Cárdenas LM, Bhogal A, Chadwick DR, *et al.*, (2019). Nitrogen use efficiency and nitrous oxide  
497 emissions from five UK fertilised grasslands. *Sci. Total Environ.* 661, 696-710.
- 498 32. Jenkinson, D. S. (1977). The nitrogen economy of the Broadbalk experiments. I. Nitrogen  
499 balance in the experiments. *Rothamsted Experimental Station Report for 1976*, Part 2, pp. 103-  
500 109.
- 501 33. Powlson D.S., Pruden G., Johnston A.E., *et al.* (1986). The nitrogen cycle in the Broadbalk  
502 Wheat Experiment: recovery and losses of <sup>15</sup>N-labelled fertilizer applied in spring and inputs of  
503 nitrogen from the atmosphere. *J. Agric. Sci., Camb.* 107, 591-609.
- 504 34. Addiscott, T., Powlson, D. (1992). Partitioning losses of nitrogen fertilizer between leaching and  
505 denitrification. *J. Agric. Sci., Camb.* 118, 101-107.
- 506 35. Skinner C., Gattinger A., Muller A., *et al.*, (2014). Greenhouse gas fluxes from agricultural soils  
507 under organic and non-organic management — a global meta-analysis. *Sci. Total Environ.* 468-  
508 469, 553-563.
- 509 36. Körschens M., Albert E., Armbruster M., *et al.*, (2013). Effect of mineral and organic  
510 fertilization on crop yield, nitrogen uptake, carbon and nitrogen balances, as well as soil organic  
511 carbon content and dynamics: results from 20 European long-term field experiments of the  
512 twenty-first century. *Arch. Agron. Soil Sci.* 59, 1017-1040.
- 513 37. Oelofse M., Markussen B., Knudsen L., *et al.*, (2015). Do soil organic carbon levels affect  
514 potential yields and nitrogen use efficiency? An analysis of winter wheat and spring barley field  
515 trials. *Euro. J. Agron.* 66, 62-73.
- 516 38. Hijbeek R., van Ittersum M.K., ten Berge H.F.M., *et al.*, (2017). Do organic inputs matter – a  
517 meta-analysis of additional yield effects for arable crops in Europe. *Plant Soil* 411, 293-303.
- 518 39. Huang J., Hartemink A.E., Kucharik C.J. (2021). Soil-dependent response of US crop yields to  
519 climate variability and depth to groundwater. *Agric. Syst.* 190, 103085
- 520 40. Kane D.A., Bradford M.A., Fuller E., *et al.*, (2021). Soil organic matter protects US maize yields  
521 and lowers insurance payouts under drought. *Environ. Res. Lett.* 16, 044018.
- 522 41. Macholdt J., Piepho H.-P., Honermeier B., *et al.*, (2020). The effects of cropping sequence,  
523 fertilization and straw management on the yield stability of winter wheat (1986-2017) in the  
524 Broadbalk Wheat Experiment, Rothamsted, UK. *J. Agric. Sci.* 158, 65-79.
- 525 42. Powlson, D. S., Poulton, P. R., Glendining, M., *et al.* (2022). Is it possible to attain the same soil  
526 organic matter content in arable agriculture soils as under natural vegetation? *Outlook on*  
527 *Agriculture.* 51, 91-104.
- 528 43. Guenet, B, Gabrielle, B, Chenu, C, *et al.* (2020). Can N<sub>2</sub>O emissions offset the benefits from soil  
529 organic carbon storage? *Global Change Biol.* 27, 237– 256.
- 530 44. Lugato, E., Leip, A., Jones, A. (2018). Mitigation potential of soil carbon management  
531 overestimated by neglecting N<sub>2</sub>O emissions. *Nature Clim. Change* 8, 219–223.
- 532 45. Macdonald, A., Poulton, P., Clark, I., *et al.* (2018). *Guide to the Classical and Other Long-term*  
533 *experiments, Datasets and Sample Archive. Rothamsted Research*, 57 pp.
- 534 46. Vogel, H.-J., Weller, U. & Schlüter, S. (2010). Quantification of soil structure based upon  
535 Minkowski functions. *Comput. Geosci.* 36, 1236–1245.
- 536 47. Zhang X., Crawford J.W., Flavel R.J., *et al.* (2016). A multi-scale Lattice Boltzmann model for  
537 simulating solute transport in 3D X-ray micro-tomography images of aggregated porous  
538 materials. *J. Hydrol.* 541, 1020-1029.
- 539 48. Li Z., Zhang X., Wang D.I., *et al.* (2018). Direct methods to calculate the mass exchange between  
540 solutes inside and outside aggregates in macroscopic model for solute transport in aggregated  
541 soil. *Geoderma*, 320, 126-135.
- 542 49. Harrison, D.E.F., Pirt, S.J. (1967). The influence of dissolved oxygen concentration on the  
543 respiration and glucose metabolism of *Klebsiella aerogenes* during growth. *J. Gen. Microbiol.*  
544 46, 193–211.
- 545 50. Bolger, A. M., Lohse, M., Usadel, B. (2014). Trimmomatic: A flexible trimmer for Illumina  
546 sequence data. *Bioinformatics* 30, 2114–2120.
- 547 51. Buchfink, B., Xie, C., Huson, D.H. (2015). Fast and sensitive protein alignment using  
548 DIAMOND. *Nature Meth.* 12, 59–60.

- 549 52. Huson, D.H., Beier S., Flade I., *et al.* (2016). MEGAN Community Edition—interactive  
550 exploration and analysis of large-scale microbiome sequencing data. *PLoS Comput. Biol.* 12(6),  
551 e1004957.
- 552 53. Kanehisa, M., Sato, Y., Kawashima, M., *et al.*, (2015). KEGG as a reference resource for gene  
553 and protein annotation. *Nucl. Acids Res.* 44, D457–D462.
- 554 54. Bateman, E.J., Baggs, E.M. (2005). Contributions of nitrification and denitrification to N<sub>2</sub>O  
555 emissions from soils at different water-filled pore space. *Biol. Fert. Soils* 41, 379–388.
- 556 55. Liang D., Robertson G.P. (2021). Nitrification is a minor source of nitrous oxide (N<sub>2</sub>O) in an  
557 agricultural landscape and declines with increasing management intensity. *Global Change Biol.*  
558 7, 5599–5613.
- 559 56. Cowan N.J., Famulari D., Levy P.E., *et al.* (2014). Investigating uptake of N<sub>2</sub>O in agricultural  
560 soils using a high-precision dynamic chamber method. *Atmos. Meas. Tech. Discuss.* 7, 8125–  
561 8147.
- 562

## 563 **Figure and Table legends**

564

565 **Figure 1.** Trends in **A** soil organic carbon (SOC) and **B** soil total nitrogen (N<sub>tot</sub>) stocks in unmanaged  
566 woodland and grassland soils, and arable soils of the Broadbalk Winter Wheat Experiment receiving  
567 farmyard manure (FYM) annually, or inorganic fertiliser at rates of 240 kg-N ha<sup>-1</sup> yr<sup>-1</sup> as ammonium  
568 nitrate combined with phosphorus and potassium (<sup>240</sup>NPK), 144 kg-N ha<sup>-1</sup> yr<sup>-1</sup> combined with  
569 phosphorus, and potassium (<sup>144</sup>NPK), 192 kg-N ha<sup>-1</sup> yr<sup>-1</sup> with potassium but no phosphorus (<sup>192</sup>NK)  
570 and soil which has received no fertilisation (nil). Soil management is summarised in Table I.

571

572 **Figure 2.** Contrasting long-term soil management results in quantitatively different process-form  
573 states. **A** - Geometric mean functional relationship between soil organic carbon (SOC) and total  
574 nitrogen (N<sub>tot</sub>) spanning the years 1843 – 2015 measured in farmyard manure (FYM)-amended,  
575 inorganically-fertilised (<sup>240</sup>NPK, <sup>144</sup>NPK, <sup>192</sup>NK) and unfertilised (nil) arable soils of the Broadbalk  
576 Winter Wheat Experiment, and unmanaged (woodland and grassland) soils. Slope = 0.088  
577 (bootstrapped 95% confidence interval, 0.085 – 0.091),  $t = 60.7$ ,  $p = 6.5 \times 10^{-63}$ ;  $\rho = 0.990$ ,  $t = 60.1$ ,  $p =$   
578  $1.3 \times 10^{-62}$ . **B** – FYM-amended, <sup>144</sup>NPK, <sup>192</sup>NK and PK arable soils, and woodland and grassland  
579 unmanaged soils are described by a combination of the connectivity of pore space, established from  
580 X-ray computed tomography, and simulated saturated hydraulic conductivity ( $K$ , in units of  $\mu\text{m s}^{-1}$ )—  
581 a measure of capacity, representing the maximum potential movement of resources through pore  
582 networks to organisms. Data point size is proportional to SOC stocks (Mg ha<sup>-1</sup>) in each soil, shown in  
583 Supplementary Fig 1A. **C** - Process-form states control anoxia within the same soils. Low-SOC, low-  
584 connected porosity soils (inorganically fertilised and unfertilised arable soils <sup>144</sup>NPK, <sup>192</sup>NK and nil)  
585 contain large volumes of anoxic microsites. Across a range of matric potential ( $\psi_m$ ), the predicted  
586 volume of anoxic sites is consistently larger in these soils than high-SOC, high-connected porosity  
587 soil (FYM-amended arable, and grassland and woodland soils). Anoxic pore space was modelled  
588 under conditions of relatively low microbial respiration,  $k' = 8.5 \times 10^{-3}$ . Key shown in **A** relates to all  
589 three figures.

590

591 **Figure 3.** Nitrogen metabolism-associated gene assemblages in farmyard manure (FYM)-amended,  
592 inorganically fertilised (<sup>144</sup>NPK, <sup>192</sup>NK and PK) arable of the Broadbalk Winter Wheat Experiment,  
593 and unmanaged (woodland and grassland) soils determined from shotgun metagenomics. **Left** –  
594 heatmap representation and bi-hierarchical clustering of gene orthologs (vertical clustering) and soil  
595 management (horizontal clustering) based upon centred-log ratio scaled ortholog relative abundance.  
596 Genes are identified by their KEGG ortholog (K) number and gene name. The largest log<sub>2</sub>-fold  
597 difference between soils is shown together with a measure of significance of the difference  
598 determined using Wald's test and Benjamini-Hochberg false discovery rate correction ( $p_{\text{adj}}$ ). **Right** –  
599 association of individual genes with nitrogen metabolism-related functional units of gene sets  
600 associated with metabolic pathways (modules). Closed circles indicate genes for which a significant

601 difference in abundance between soils was identified, open circles indicate genes for which no  
602 significant difference was observed. The KEGG ontology does not discriminate between the genes  
603 *amoABC* associated with ammonia oxidation and *pmoABC* associated with methane oxidation.  
604

605 **Figure 4.** Adjusted mean estimates of nitrous oxide (N<sub>2</sub>O) emissions from farmyard manure (FYM)-  
606 amended and inorganically fertilised (<sup>240</sup>NPK, <sup>144</sup>NPK, <sup>192</sup>NK and PK) soils of the Broadbalk Winter  
607 Wheat Experiment measured between April and November 2019. Error bars represent the standard  
608 error of the mean, *t* and probabilities (*p*) indicate the results of Holm-Šidák *a priori* contrasts of FYM,  
609 <sup>144</sup>NPK, <sup>192</sup>NK and PK mean N<sub>2</sub>O emissions to <sup>240</sup>NPK emissions.  
610

611 **Figure 5.** Nonequilibrium nitrogen use efficiency of farmyard manure (FYM)-amended and  
612 inorganically fertilised (<sup>240</sup>NPK, <sup>192</sup>NPK, <sup>144</sup>NPK and PK) soils of the Broadbalk Winter Wheat  
613 Experiment between 2000 and 2015 indicates divergent allocation of *A* – absolute nitrogen inputs to  
614 arable systems and *B* - nitrogen inputs supporting 1 Mg of grain production, between grain, straw, soil  
615 and lost pools. Small increases in nitrogen soil stocks observed for inorganic plots could be due to  
616 measurement error, as these systems are assumed to have reached steady states. *C* – Grain yields for  
617 inorganically fertilised and FYM-amended soils for the same period. Box plots show interpolated  
618 25% and 75% quartiles, the median is represented as a horizontal line. Whiskers indicate minimum  
619 and maximum values. Each treatment mean is represented by a X, the line connects treatment means.  
620 Results of analysis of variance (ANOVA) are shown together with estimates of treatment effect size  
621 ( $\omega^2$ ) upon yield, calculated as  $(SS_{bg} - df_{bg} \cdot MS_{wg}) / (SS_{total} + MS_{wg})$  where SS indicates the sum of  
622 squares, df the degree of freedom, MS the mean square and the subscripts bg and wg indicate  
623 between-group and within-group respectively. *Post hoc* pairwise comparisons indicate that the mean  
624 PK grain yield was significantly lower than the means of all other treatments (smallest difference,  $Q =$   
625  $11.7$ ,  $p = 2 \times 10^{-12}$ ). FYM mean grain yield was significantly lower than the mean yields of both the  
626 <sup>192</sup>NPK and <sup>240</sup>NPK treatments (smallest difference,  $Q = 4.2$ ,  $p = 0.033$ ). There was no significant  
627 difference between the mean grain yields of FYM and <sup>144</sup>NPK treatments.  
628

629 **Table I.** Fertility management associated with arable soils of the Broadbalk Winter Wheat  
630 Experiment and associated unmanaged soils used in various aspects of this study.  
631

632 **Table II.** Topology-related parameters derived directly from binary images generated from X-ray  
633 computed tomography of aggregates from farmyard manure (FYM)-amended and inorganically  
634 fertilized (<sup>144</sup>NPK, <sup>192</sup>NK and PK) arable soils of the Broadbalk Winter Wheat Experiment and  
635 unmanaged woodland and grassland (total and connected porosity) and estimates of permeability (*k*),  
636 effective diffusion coefficient of oxygen (*D<sub>e</sub>*) which is normalised by dividing the diffusion  
637 coefficient of oxygen in water without pore constraints, and hydraulic conductivity (*K*) of the soil  
638 pore networks derived from lattice Boltzman simulation (and where  $K = gk/\nu$  where *g* is the  
639 gravitational constant, *k* the permeability, and  $\nu$  the viscosity of water). The mean associated with  
640 each parameter is provided together with the standard error of the mean in parentheses. Results of  
641 analysis of variance (ANOVA) are shown together with estimates of treatment effect size ( $\omega^2$ ) for  
642 each parameter, calculated as  $(SS_{bg} - df_{bg} \cdot MS_{wg}) / (SS_{total} + MS_{wg})$  where SS indicates the sum of squares,  
643 df the degree of freedom, MS the mean square and the subscripts bg and wg indicate between-group  
644 and within-group respectively.  
645

646 **Supplementary Figure 1. A** - Soil organic carbon (SOC) stocks for the years 1966 – 2015  
647 measured in farmyard manure (FYM)-amended, inorganically fertilised (<sup>240</sup>NPK, <sup>144</sup>NPK, <sup>192</sup>NK and  
648 PK) and unfertilised (nil) arable soils of the Broadbalk Winter Wheat Experiment and unmanaged  
649 grassland soil. **B** - Soil total nitrogen (N<sub>tot</sub>) stocks for the same period and treatments. Box plots  
650 indicate the interpolated 25% and 75% quartiles with the median represented as a horizontal line.  
651 Whiskers indicate minimum and maximum values. Results of analysis of variance (ANOVA) are  
652 shown together with estimates of treatment effect size ( $\omega^2$ ) upon SOC and N<sub>tot</sub>, calculated as  $(SS_{bg} -$   
653  $df_{bg} \cdot MS_{wg}) / (SS_{total} + MS_{wg})$  where SS indicates the sum of squares, df the degree of freedom, MS the  
654 mean square and the subscripts bg and wg indicate between-group and within-group respectively.



655

656 **Supplementary Figure 2.** Mean estimates ( $n = 3$ ) of nitrous oxide ( $\text{N}_2\text{O}$ ) emissions from farmyard  
657 manure (FYM)-amended and inorganically fertilised ( $^{240}\text{NPK}$ ,  $^{144}\text{NPK}$ ,  $^{192}\text{NK}$  and PK) soils of the  
658 Broadbalk Winter Wheat Experiment measured in 2019. Emissions were measured discontinuously  
659 on the dates shown using in-field static chambers. Daily precipitation measured on a 254-mm  
660 diameter rain gauge located 500 m east of the field experiment together with the potential soil  
661 moisture deficit (PSMD) are also shown.

662

663 **Supplementary Figure 3.** Nonequilibrium nitrogen use efficiency of farmyard manure (FYM)-  
664 amended and inorganically fertilised ( $^{240}\text{NPK}$ ,  $^{192}\text{NPK}$ ,  $^{144}\text{NPK}$  and PK) treatments of the Broadbalk  
665 Winter Wheat Experiment between 2000 and 2015. The proportion of total nitrogen inputs derived  
666 from ammonium nitrate fertiliser or FYM, associated with seed grain and atmospheric deposition  
667 allocated to harvested grain and straw, and soil and lost pools.

668

Figure 1.

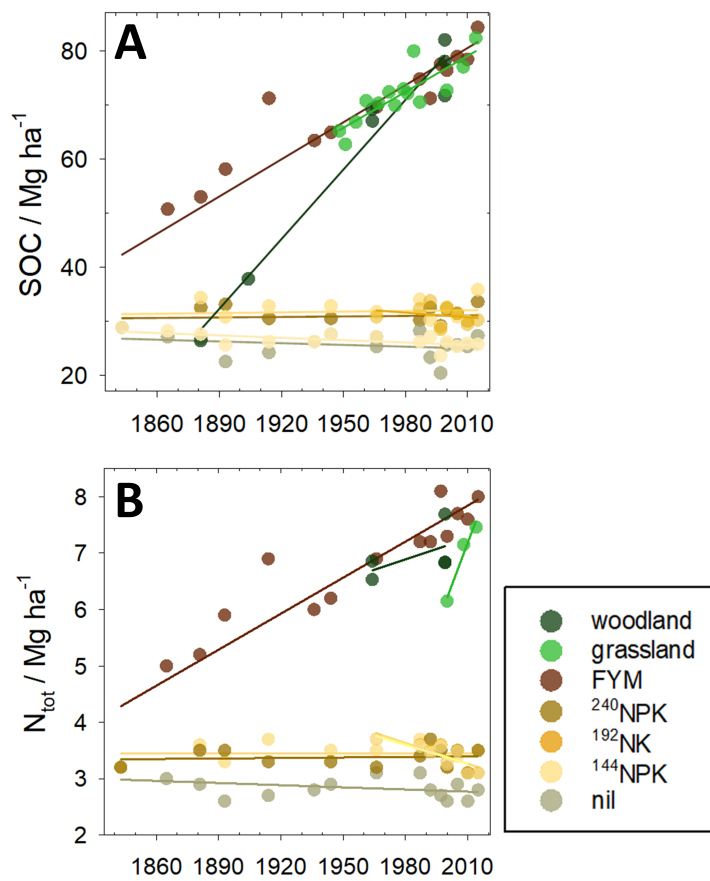
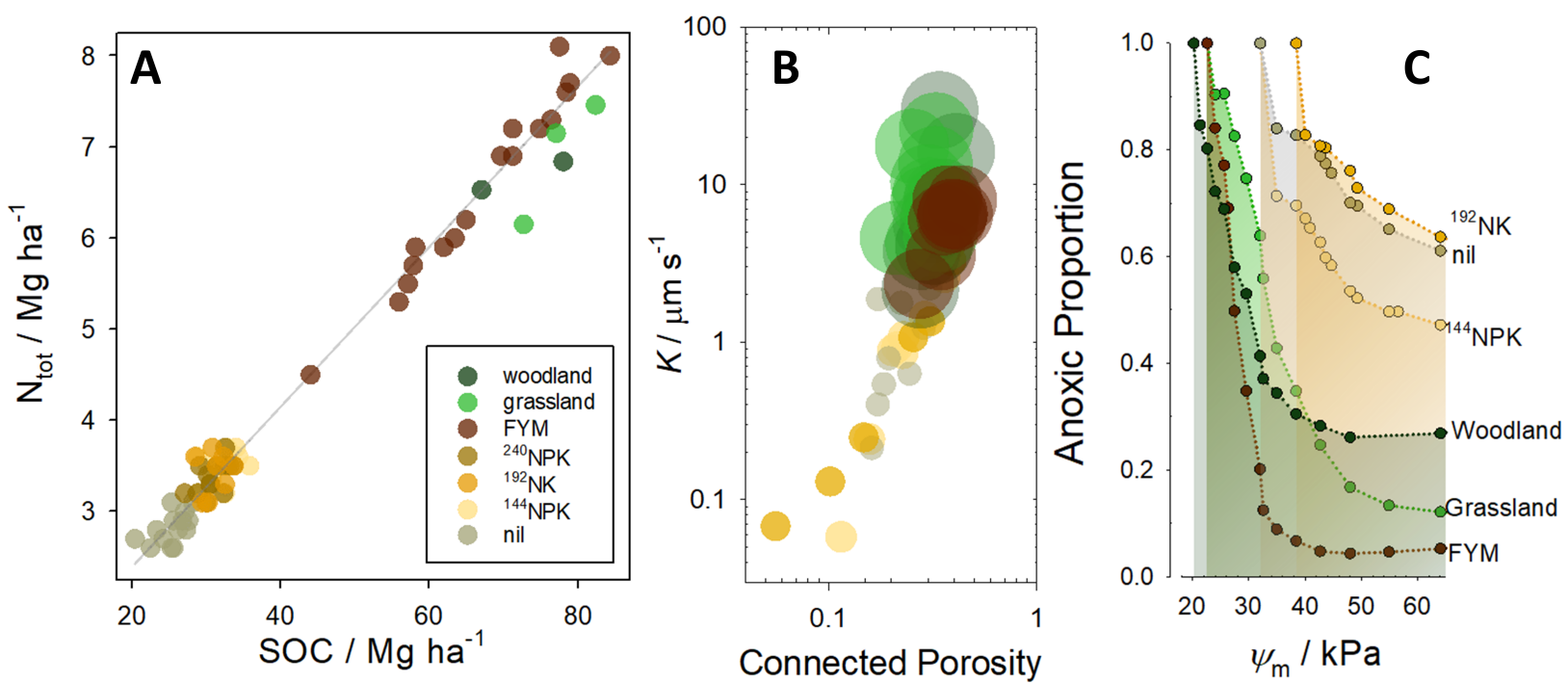


Figure 2.



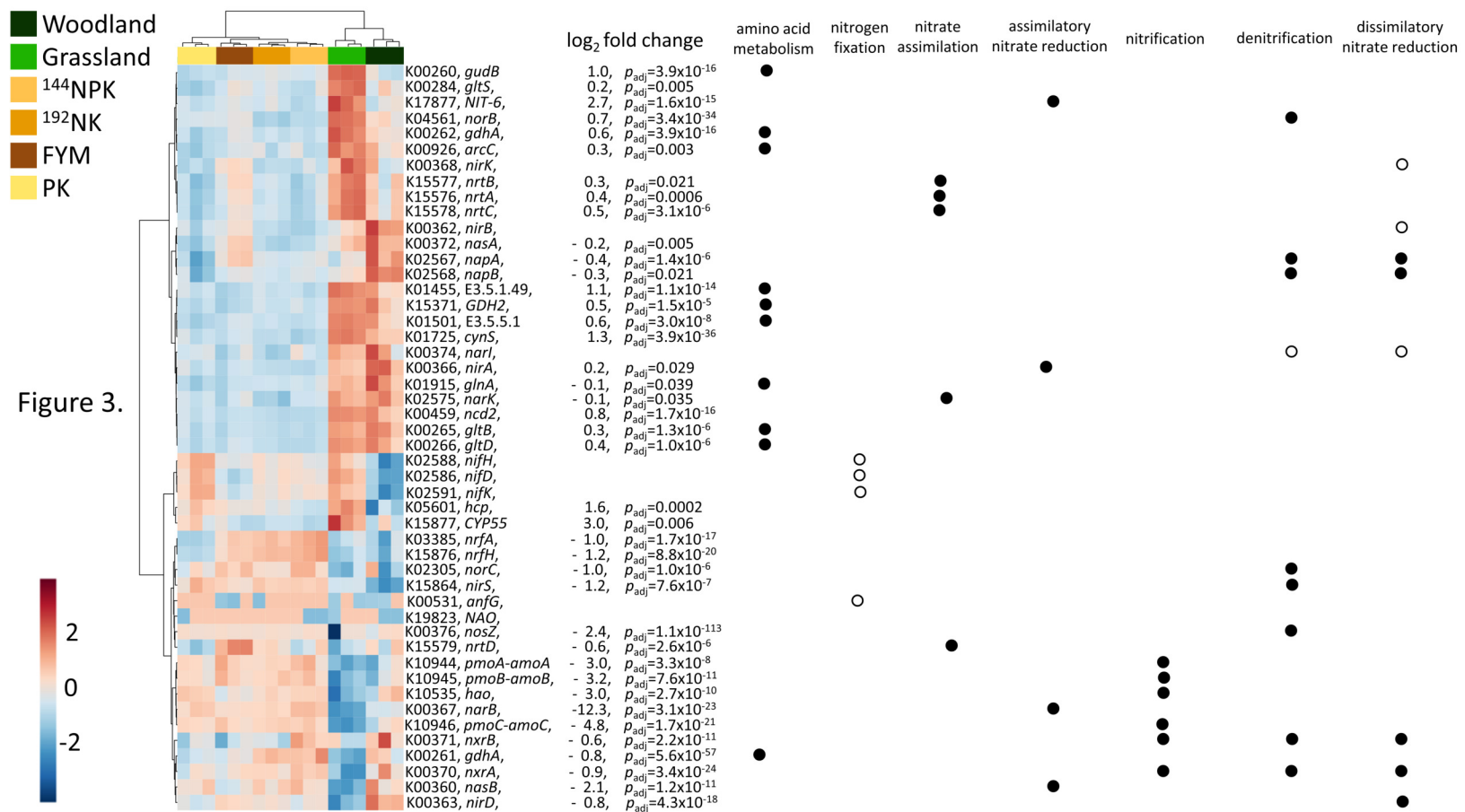


Figure 4.

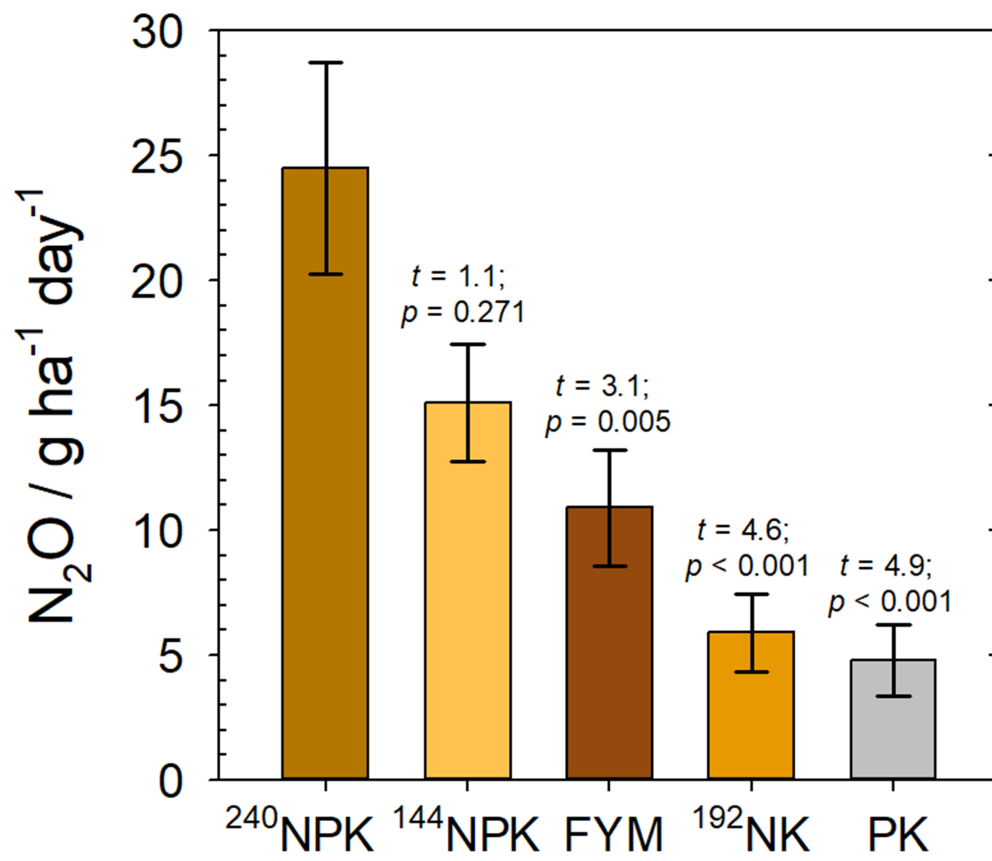


Figure 5.

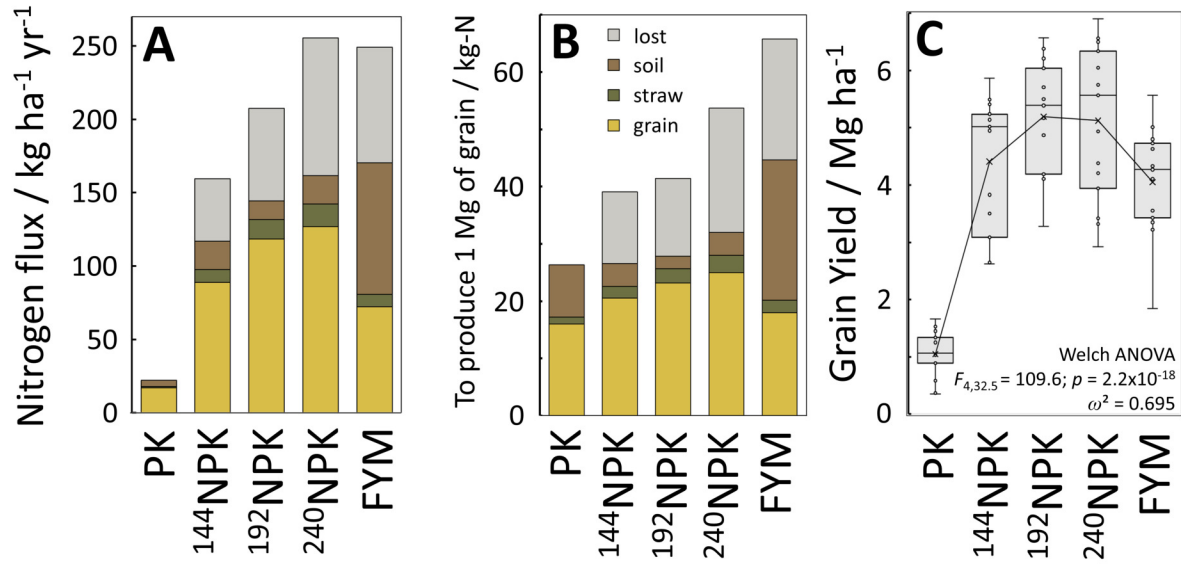


Table I.

Treatment	Annual fertility management	Designation
Arable, composted farmyard manure	35 Mg ha <sup>-1</sup> since 1843	FYM
Arable, 240 kg-N ha <sup>-1</sup> inorganic fertiliser <sup>a</sup>	240 kg-N ha <sup>-1</sup> since 1985; (144 kg-N ha <sup>-1</sup> between 1852 and 1984)	<sup>240</sup> NPK
Arable, 192 kg-N ha <sup>-1</sup> , inorganic fertiliser <sup>a</sup>	192 kg-N ha <sup>-1</sup> since 1968	<sup>192</sup> NPK
Arable, 144 kg-N ha <sup>-1</sup> inorganic fertiliser <sup>a</sup>	144 kg-N ha <sup>-1</sup> since 1852	<sup>144</sup> NPK
Arable, inorganic fertiliser <sup>a</sup> , no phosphorus	No triple superphosphate additions since 1968; (96 kg-N ha <sup>-1</sup> between 1968 and 2001; 192 kg-N ha <sup>-1</sup> since)	<sup>192</sup> NK
Arable, inorganic fertiliser <sup>a</sup> , no nitrogen	No ammonium nitrate additions since 1852	PK
Arable, unfertilised	No fertiliser additions since 1852	nil
Grassland	None, grassland since 1838	grassland
Woodland	None, woodland since 1882	woodland

<sup>a</sup> – unless stated otherwise, inorganic fertiliser included inorganic nitrogen as ammonium nitrate, 90 kg-K ha<sup>-1</sup> as K<sub>2</sub>SO<sub>4</sub>, 35 kg-P ha<sup>-1</sup> as triple superphosphate [Ca(H<sub>2</sub>PO<sub>4</sub>)<sub>2</sub>·H<sub>2</sub>O], and 12 kg-Mg ha<sup>-1</sup> as kieserite (MgSO<sub>4</sub>·H<sub>2</sub>O)

Table II.

	<b>Total Porosity (<math>P_t</math>) / %</b>	<b>Connected Porosity (<math>P_c</math>) / %</b>	<b>Permeability (<math>k</math>) / <math>\mu\text{m}^2</math></b>	<b>Diffusion Coefficient (<math>D_e</math>)'</b>	<b>Hydraulic Conductivity (<math>K</math>) / <math>\mu\text{m s}^{-1}</math></b>
	Welch ANOVA; $F_{5,20.8} = 14.1$ , $p = 4.5 \times 10^{-6}$	Welch ANOVA; $F_{5,20.7} = 14.2$ , $p = 4.3 \times 10^{-6}$	Welch ANOVA; $F_{5,21} = 36.5$ , $p = 1.4 \times 10^{-9}$	ANOVA; $F_{5,47} = 19.5$ , $p = 1.8 \times 10^{-10}$	Welch ANOVA; $F_{5,21} = 15.8$ , $p = 2.1 \times 10^{-6}$
	$\omega^2 = 0.467$	$\omega^2 = 0.459$	$\omega^2 = 0.775$	$\omega^2 = 0.636$	$\omega^2 = 0.361$
<b>woodland</b>	33.1 (1.3)	32.8 (1.4)	0.396 (0.131)	0.278 (0.020)	8.86 (2.94)
<b>grassland</b>	31.0 (1.2)	30.8 (1.2)	1.13 (0.089)	0.254 (0.015)	9.61 (1.61)
<b>FYM</b>	37.7 (1.6)	37.5 (1.6)	0.265 (0.028)	0.335 (0.023)	5.92 (0.62)
<b><math>^{144}\text{NPK}</math></b>	23.6 (2.4)	22.4 (2.7)	0.045 (0.012)	0.135 (0.016)	1.01 (0.27)
<b><math>^{192}\text{NK}</math></b>	24.9 (4.5)	23.4 (5.1)	0.065 (0.027)	0.151 (0.032)	1.45 (0.60)
<b>PK</b>	22.6 (1.7)	21.6 (1.8)	0.048 (0.011)	0.129 (0.014)	1.07 (0.24)